molecular pharmaceutics

ARTICLE

pubs.acs.org/molecularpharmaceutics

Development of Novel Efficient SIN Vectors with Improved Safety Features for Wiskott–Aldrich Syndrome Stem Cell Based Gene Therapy

Inés Avedillo Díez,[†,‡,§] Daniela Zychlinski,[‡,∥] Emanuele G. Coci,[†,‡,∥,⊥] Melanie Galla,[‡,∥] Ute Modlich,[∥] Ricardo A. Dewey,[†,§] Adrian Schwarzer,[∥] Tobias Maetzig,[‡,∥] Nonsikelelo Mpofu,[#] Elmar Jaeckel,[#] Kaan Boztug,[†,‡,⊥] Christopher Baum,[‡,∥,⊥] Christoph Klein,[*,†,‡,⊥] and Axel Schambach[*,‡,∥,⊥]

[†]Department of Pediatric Hematology/Oncology, [∥]Institute of Experimental Hematology, [‡]Excellence Cluster REBIRTH, [⊥]Integrated Research and Treatment Center Transplantation, and [#]Department of Gastroenterology, Hepatology and Endocrinology, Hannover Medical School, Germany

Supporting Information

ABSTRACT: Gene therapy is a promising therapeutic approach to treat primary immunodeficiencies. Indeed, the clinical trial for the Wiskott–Aldrich Syndrome (WAS) that is currently ongoing at the Hannover Medical School (Germany) has recently reported the correction of all affected cell lineages of the hematopoietic system in the first treated patients. However, an extensive study of the clonal inventory of those patients reveals that *LMO2*, *CCND2* and *MDS1/EVI1* were preferentially prevalent. Moreover, a first leukemia case was observed in this study, thus reinforcing the need of developing safer vectors for gene transfer into HSC in general. Here we present a novel self-inactivating (SIN) vector for the gene therapy of WAS that combines improved safety features. We used the elongation factor 1 alpha (EFS) promoter, which has been extensively evaluated in terms of safety profile, to drive a codon-optimized human *WASP* cDNA. To test vector performance in a more clinically relevant setting, we transduced murine HSPC as well as human CD34+ cells and also analyzed vector efficacy in their differentiated myeloid progeny. Our results show that our novel vector generates comparable WAS protein levels and is as effective as the clinically used LTR-driven vector. Therefore, the described SIN vectors appear to be good candidates for potential use in a safer new gene therapy protocol for WAS, with decreased risk of insertional mutagenesis.

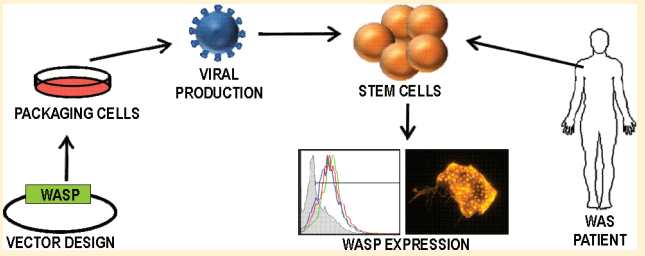

KEYWORDS: gene therapy, self-inactivating, codon-optimization

INTRODUCTION

Wiskott–Aldrich syndrome (WAS) is an X-linked primary immunodeficiency disorder characterized by thrombocytopenia, recurrent infections, eczema and an increased incidence of autoimmune manifestations.[1] WAS is caused by mutations in the *WAS protein* (*WASP*) gene which encodes for a key regulator of actin polymerization expressed exclusively in cells of hematopoietic origin.[2] Defective WASP expression causes complex immunologic abnormalities affecting T cells, B cells, natural killer cells, dendritic cells, macrophages and granulocytes, respectively.[3] Patients with classical WAS usually die within the first decades of their life,[4] unless treated by allogenic hematopoietic stem cell transplantation (HSCT).[5] However, HSCT can be associated with severe morbidity and mortality secondary to infections, graft-versus-host-disease (GvHD), nonengraftment and post-transplant lymphoproliferative syndrome,[6] especially in patients transplanted with HSC from HLA-mismatched donors and in patients transplanted at an age older than five years.[7]

In disorders caused by mutations of single genes, gene therapy is an attractive concept to specifically revert the molecular defect underlying the disease. This holds true in particular for hematopoietic diseases where target stem cells are accessible with relative ease for *in vitro* manipulation and subsequent reinfusion.[8] The first human disease treated successfully by gene therapy was X-linked severe combined immunodeficiency (X-SCID),[5] soon followed by reports of successful treatment of ADA-SCID[9] and chronic granulomatous disease (CGD),[10] and more recently, the Wiskott–Aldrich syndrome.[11] In spite of the documented clinical benefit, the current technology is far from being perfect. Five out of 20 patients treated in two X-SCID clinical trials with transduced HSC developed malignant clonal disorders presenting clinically as leukemia/lymphoma,[12,13] and two adult patients with CGD developed a myelodysplastic syndrome characterized

Special Issue: Emerging Trends in Gene- and Stem-Based Combination Therapy

Received: March 15, 2011
Accepted: August 18, 2011
Revised: August 5, 2011
Published: August 18, 2011

by monosomy 7.[14] Also a first case of leukemia, possibly triggered by insertional upregulation of a neighboring *LMO2* allele, was observed in one patient of the series of WAS patients we have treated so far with a gammaretroviral LTR-driven vector.[15,16] This has fueled the need to advance the development of improved vector systems.

U3-deleted, so-called "self-inactivating" (SIN) vectors, confer a reduced risk for insertional mutagenesis and secondary cancer[17−19] because the promoter/enhancer regions have been deleted from the LTR. Both lentivirus- and gammaretrovirus-based vectors have been tested in preclinical studies.[20,21] Lentiviruses (LV), with their tendency to insert the genetic cargo into transcribed genes, have been shown to be potentially less genotoxic than gammaretroviruses (RV), which show a preference to integrate close to transcriptional start sites and regulatory gene regions.[22,23] However, the latest advances in the field indicate that altering the promoter/enhancer elements of the vector has a greater effect on safety than the retroviral insertion pattern[24] and that the insertional gene activation is determined by the characteristics of the transcriptional regulatory elements carried by the vector, thus it is in part independent of the vector type.[25] The selection of the internal promoter is an important point to consider, given that cellular promoters show a reduced risk of activating neighboring proto-oncogenes in comparison to internal promoters of viral origin.[18] The potency and increased safety of the described gammaretroviral and lentiviral SIN vector backbones have already been described in previous studies.[16−18,26]

We here present a gammaretroviral (and lentiviral) SIN-vector with redesigned backbone architecture. We included an improved version of a woodchuck post-transcriptional regulatory element (wPRE).[27] Moreover, the coding sequence of the *WASP* transgene has been optimized, resulting in more stable RNA, which allows protein expression levels above the therapeutic threshold under the control of the human elongation factor 1-α short (EFS) promoter, a cellular promoter with a constitutive activity in hematopoietic stem/progenitor cells (HSPC).[18] Importantly, this study also provides evidence for the efficacy of this novel vector in WASP deficient CD34+ cells, the target cell population for gene therapy. Therefore, this vector appears to be a good candidate vector to pursue the development of a safer gene therapy protocol for WAS, with greatly decreased risk of insertional mutagenesis.

MATERIALS AND METHODS

Viral Vectors and Vector Production. An advanced generation, self-inactivating (SIN) gammaretroviral vector,[27,28] SRS11.EFS.WASP.iresGFP.pre (R.EFS.W.iG), was constructed to express a full-length human *WASP* cDNA (W) under the control of the human elongation factor 1-α short (EFS) promoter (Figure 1). *WASP* (W) was cloned into *Xba*I and *Sal*I unique restriction sites, and iresGFP (iG) was cloned downstream into a unique *Bam*HI restriction site (Figure 1). To generate the lentiviral counterpart, the same expression cassette was cloned through a *Not*I (blunted by Klenow polymerase)/*Spe*I restriction into the *Xho*I (blunted by Klenow polymerase)/*Spe*I sites of pRRL.PPT.SF.GFP.pre*, a standard third generation lentiviral vector.[29,30] The resulting vector was named pRRL.PPT.EFS.WASP.iresGFP.pre (L.EFS.W.iG) (Figure 1). The EFS internal promoter was substituted by the spleen focus-forming virus (SFFV) U3 promoter/enhancer to generate SRS11.SFFV.WASP.iresGFP.pre (R.SF.W.iG) and pRRL.PPT.SFFV.WASP.iresGFP.pre (L.SF.W.iG) (Figure 1). The substitution of *WASP* cDNA (W) by a codon-optimized *WASP* (Wco) sequence (Epoch Biolabs Inc., Texas, USA) was carried out in all vectors through *Age*I/*Xba*I and *Sal*I restriction sites, thus generating SRS11.EFS.WASPco.iresGFP.pre (R.EFS.Wco.iG), SRS11.SFFV.WASPco.iresGFP.pre (R.SF.Wco.iG), pRRL.PPT.EFS.WASPco.iresGFP.pre (L.EFS.Wco.iG) and pRRL.PPT.SFFV.WASPco.iresGFP.pre (L.SF.Wco.iG), respectively (Figure 1). All SIN vectors contain the safety improved woodchuck hepatitis virus post-transcriptional regulatory element (PRE*)[31] downstream of iG (iresGFP). The cloning of the CMMP.WASP.iresGFP (CMMP.W.iG) vector containing intact myeloproliferative sarcoma virus (MPSV) LTRs has been described previously.[24,32]

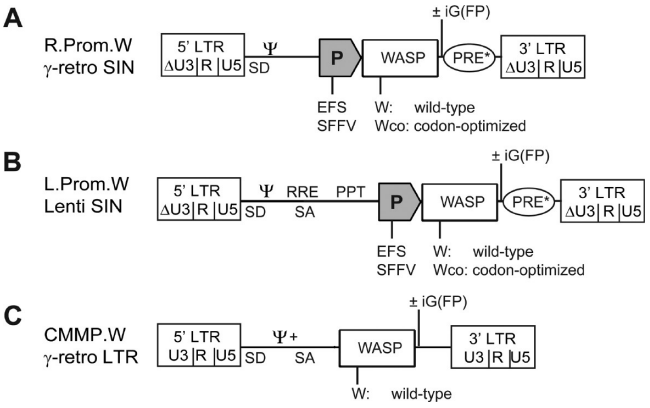

Figure 1. Design of viral vectors used in this study. (A) The proviral self-inactivating (SIN) gammaretroviral vectors contain long terminal repeat sequences (LTRs) on both ends, devoid of LTR promoter/enhancer sequences after reverse transcription. The elongation factor 1-α (EFS) or the spleen focus forming virus (SFFV) are used as internal promoters (Prom, P) to drive the WASP cDNA (WASP) either wild-type (W) or codon optimized (Wco). Optionally, this is followed by an internal ribosome entry site (i), and the green fluorescent protein (G) as a marker. Furthermore, the vectors include the safety-improved woodchuck hepatitis virus post-transcriptional regulatory element (PRE*), a splice donor (SD), and the packaging signal (Ψ). (B) The SIN-lentiviral counterparts include the Rev responsive element (RRE), and the central polypurine tract (PPT) in addition to the above-described elements. (C) The gammaretroviral LTR-driven vector used in the Hannover clinical trial (CMMP) exhibits intact myeloproliferative sarcoma virus (MPSV) long terminal repeats (LTRs), an extended packaging signal (Ψ+) and a splice acceptor (SA); other elements, see description above.

Retroviral cell-free vector supernatants were generated by transient cotransfection of 293T packaging cells with each transfer vector, together with packaging constructs coding for the gag-pol proteins (for lentiviral, pcDNA3.GP.4xCTE; for gammaretroviral, pcDNA3.MLVgp) and the ecotropic, GALV or VSV-G envelope, as previously described.[25] To produce lentiviral vectors, a RSV-Rev containing plasmid was additionally cotransfected. Viral titers were determined by flow cytometry on HT1080 and SC1 fibroblasts, respectively, and supernatants stored at −80 °C until use.

Patients. All experiments were performed upon informed consent/assent of patients or legal representatives. The study protocol was approved by the institutional review board (IRB) at Hannover Medical School.

Cell Lines and Primary Cultures. 293T, HT1080 and SC-1 cells were grown in DMEM (Biochrom, Berlin, Germany) supplemented

with 10% fetal calf serum (PAA, Pasching, Austria), 1 mM sodium pyruvate (PAA) and 100 U/ml penicillin/streptomycin (PAA). HT1080ecat is a HT1080 derivative stably expressing the ecotropic receptor mCAT-1.

Epstein−Barr virus (EBV)-transformed B lymphoblastoid cell lines (B-LCLs) were derived from peripheral blood mononuclear cells of WAS patients after infection with B95-8 cell supernatant in the presence of cyclosporin A. Cells were maintained in RPMI-1640 medium supplemented with 10% FCS, 100 U/mL penicillin/streptomycin and 2 mM glutamine.

Bone marrow (BM) lineage-negative (Lin−) cells of untreated 129 Wasp ko (knockout) mice were isolated from complete BM by magnetic sorting using the Lineage Cell Depletion Kit (Miltenyi Biotech, Bergisch-Gladbach, Germany) following the instructions given by the manufacturer. Briefly, total BM cells were magnetically labeled with a cocktail of biotinylated antibodies against a panel of lineage antigens (CD3, B220, CD11b, Gr-1 and Ter-119) and anti-biotin MicroBeads. Lin− cells were automatically separated using an AutoMACS device (Miltenyi Biotech), aliquoted and cryopreserved until usage. Cells were grown in StemSpan HS2000 medium (CellSystems, St Katharinen, Germany) containing 100 U/mL penicillin/streptomycin, 2 mM glutamine (Biochrom), 50 ng/mL murine stem cell factor (SCF), 100 ng/mL hFlt-3 ligand, 100 ng/mL hIL-11 and 10 ng/mL mIL-3 (all PeproTech, London, U.K.) at a density of $1-5 \times 10^5$ cells/mL, unless otherwise specified. For Figure 5D−F Lin− cells were cultivated in IMDM supplemented with 10% FCS, 100 U/mL penicillin/streptomycin, 2 mM glutamine, 50 ng/mL SCF, 20 ng/mL mTPO, 50 ng/mL hFlt3L and 10 ng/mL mIL3 and 20 μg/mL meropenem.

CD34+ cells were purified from human BM mononuclear cells of healthy individual donors and WAS patients using immunomagnetic beads as described by the manufacturer (Miltenyi Biotec). Separation was performed using an AutoMACS device (Miltenyi Biotec) following the manufacturer's instructions. CD34+ cells were cultured in StemSpan serum-free medium (StemCell Technologies, Inc.) supplemented with 100 U/mL penicillin/streptomycin, 2 mM glutamine, 100 ng/mL human SCF, 100 ng/mL human Flt-3 ligand, and 20 ng/mL human thrombopoietin (TPO) (PeproTech, London, U.K.).

Viral Transduction. Transduction of cells was performed on RetroNectin-coated (10 g/cm^2; TaKaRa, Otsu, Japan) suspension culture dishes preloaded with viral supernatant. Viral preloading was carried out by centrifugation of supernatant at 800*g* for 30 min at 4 °C. B-LCL were transduced with GALV-pseudotyped viruses at MOI = 1.

Lin− and CD34+ cells were expanded for two days prior to transduction. On day three, cells were transduced with ecotropic or GALV-pseudotyped viruses, respectively, by incubation on viral preloaded suspension culture dishes. Virus preloading was carried out on RetroNectin-coated dishes, as indicated above. Transduced cells were incubated for expansion for 3 to 5 days before proceeding to further experiments.

Detection of WASP by Intracellular Immunofluorescence Staining. For intracellular FACS staining, cells were treated with the Fix & Perm kit (Caltag Laboratories, Burlingame, CA, USA), as described by the manufacturer. As primary antibodies, anti-human WASP monoclonal IgG2a (Clone B-9, Santa Cruz Biotechnology, Santa Cruz, CA, USA) and mouse IgG2a isotype (Becton Dickinson GmbH, Heidelberg, Germany) were used. Goat F(ab0)2 fragment rat IgG-phycoerythrin (Immunotech) was used as a secondary antibody. Subsequently, samples were analyzed by fluorescent activated cell sorting (FACS). For immunofluorescence microscopy analysis, BM derived adherent cells from Wasp ko mice were prepared from flushed bone marrow and transduced with the depicted vector constructs. BM derived adherent cells were grown on glass coverslips. The adherent cells were washed with PBS, fixed and permeabilized with Fix&Perm solution A (Invitrogen, Darmstadt, Germany) for 20 min at room temperature. All washing steps were performed in BD Perm/Wash buffer. All antibodies were diluted in Fix&Perm solution B (Invitrogen). Cells were stained for 1 h with anti-WASP (clone B9) and washed 3 times, followed by incubation for 1 h with anti-mouse-IgG-AF546 (Molecular Probes/Invitrogen), HOECHST 33342 (CellSignaling, Danvers, MA, USA) and Phalloidin-AF635 (Molecular Probes) to detect F-actin. Adherent cells were washed and mounted with Anti-Fade-Gold (Invitrogen). Images were acquired by confocal laser scanning microscopy on a Leica DM IRB instrument equipped with a TCS SP2 AOBS scan head. Data visualization was performed using the IMARIS Software package (Bitplane AG, Zurich, Switzerland). For 3D reconstructions 10−16 0.2 μm *Z*-stacks were recorded and analyzed using IMARIS.

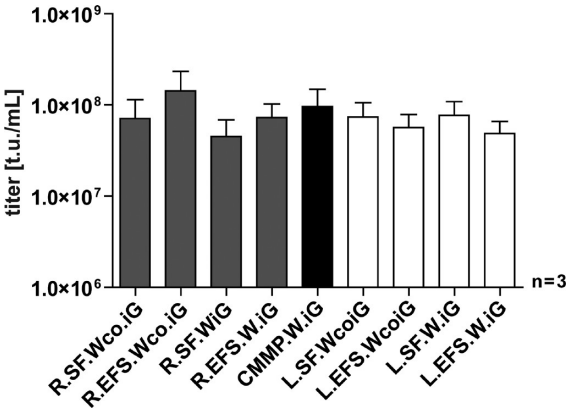

Figure 2. Titer analysis of viral supernatants used in this study. Titers are expressed in transduction units per milliliter (tu/mL) on the *Y*-axis. Bars indicate the average values obtained from three independent viral preparations (n = 3). Error bars correspond to the standard deviation. The gammaretroviral vector is abbreviated with R, the lentiviral counterpart with L.

Western Blot. Western blot analysis of WASP expression was performed as previously described.[24] The membranes were exposed either to anti-WASP monoclonal clone D-1 (Santa Cruz Biotechnology) diluted 1/400 (Figure 3E and Supplementary Figure 1 in the Supporting Information) or to anti-WASP monoclonal clone B9 (Santa Cruz Biotechnology) diluted 1/300 (Figures 5C and 5F). Horseradish peroxidase (HRP)-conjugated goat anti-mouse (Becton Dickinson GmbH) diluted 1/10000 (Figure 3E and Supplementary Figure 1 in the Supporting Information), HRP-conjugated horse anti-mouse (Cell Signaling Technology, Danvers, MA, USA) diluted 1/2000 (Figure 5F) and donkey anti-mouse fluorophore-conjugated IRDye 800CW (ROCKLAND Immunochemicals, Gilbertsville, PA, USA) diluted 1/10000 (Figure 5C) were used as secondary antibodies. Housekeeping genes that served as loading controls were detected with mouse anti-GAPDH monoclonal antibody 6C5 (Santa Cruz Biotechnology) diluted 1/10000 (Supplementary Figure 1 in the Supporting Information), rabbit polyclonal anti-Erk2 antibody

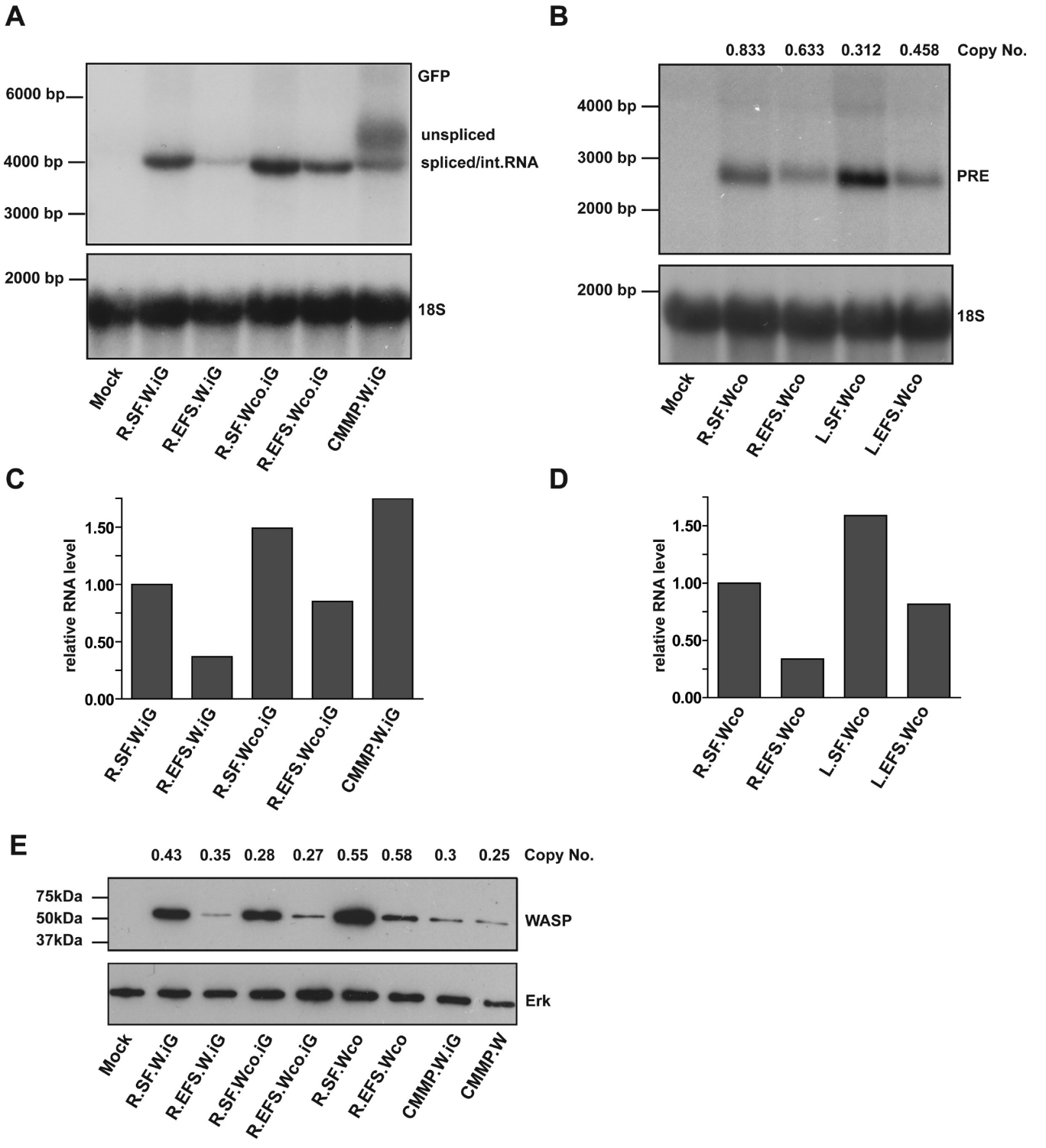

Figure 3. Characterization of newly generated vectors in terms of mRNA processing and protein expression. (A) Northern blot analysis of cell lysates from HT1080ecat cells transduced with ecotropic bicistronic retroviral vectors. Blots were probed for detection of GFP (upper) and 18S RNA (lower), respectively. (B) Northern blot analysis of HT1080ecat cells transduced with monocistronic ecotropic SIN-gammaretroviral and SIN-lentiviral vectors containing Wco as transgene. The blots were probed for PRE and 18S. Samples with similar number of viral integrations (measured by Real-Time PCR) were selected for comparison purposes. (C) Quantification of relative GFP RNA levels of samples shown in panel A. (D) Quantification of relative viral RNA levels of samples shown in panel B. (E) Western blot for detection of WASP expression in HT1080ecat cells transduced with ecotropic gammaretroviral vectors, either with or without the marker gene. CMMP is the LTR-driven vector backbone used in the Hannover WAS trial. Detection of Erk2 protein was used as loading control. The number of viral integrations per genome was calculated by Real-Time PCR (see copy number indicated above), and samples with similar copy number were selected for comparison purposes.

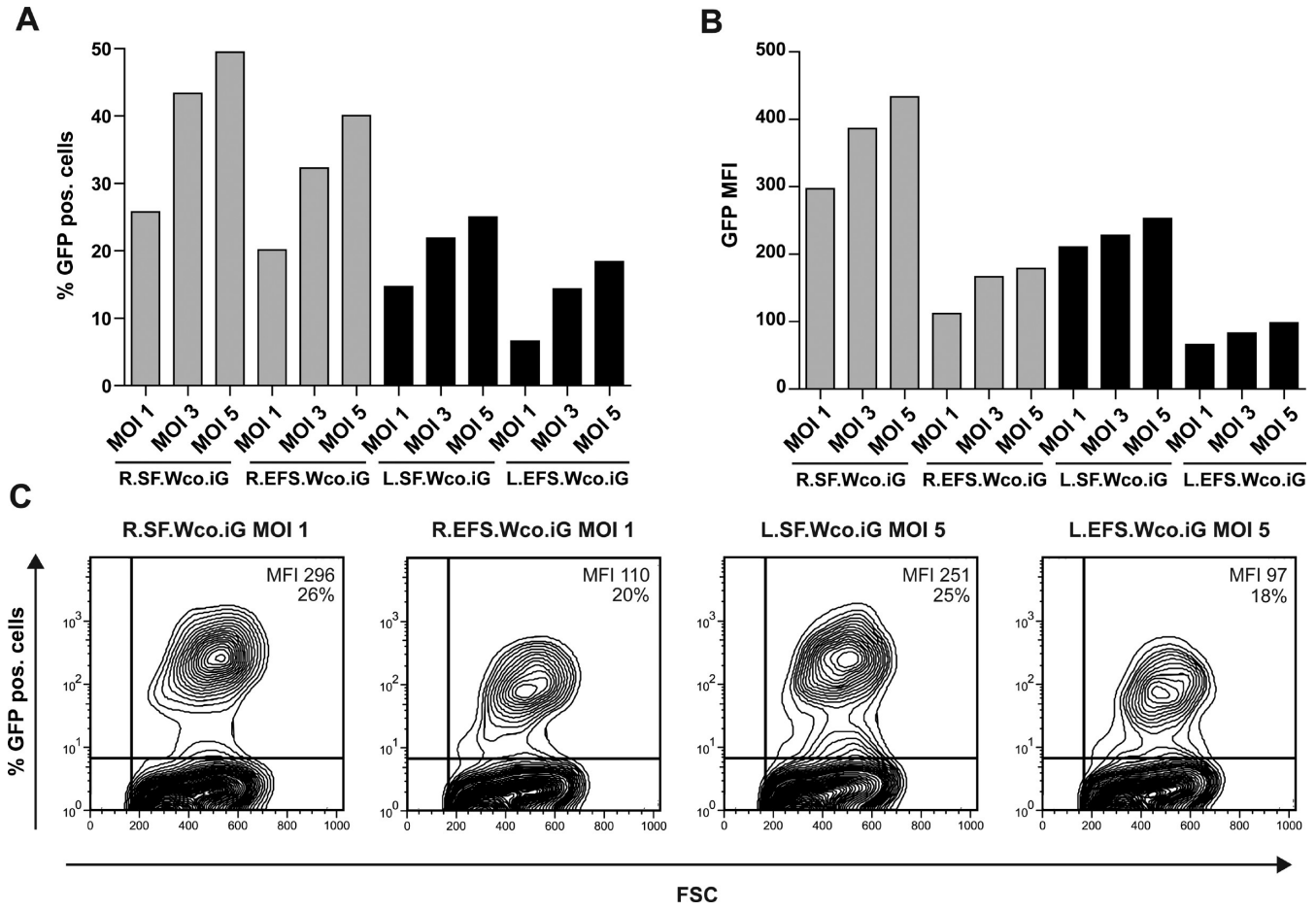

Figure 4. Transgene expression in murine Wasp ko hematopoietic precursor cells. (A) Percentage of GFP+ cells (*Y*-axis) determined three days after transduction. (B) Analyses of the mean fluorescence intensity (MFI) of the GFP expressing cells (Y-axis) for the indicated vectors. (C) Contour plots corresponding to transductions with vectors containing Wco, where similar transduction rates were obtained (between 18 and 25%). The following MFI values were obtained: 296.30 (left plot), 109.57 (midleft plot), 250.88 (midright plot), and 96.50 (right plot). Noteworthy, the MOI used to obtain these results was five times higher with lentiviral than with retroviral vectors.

(Santa Cruz Biotechnology) diluted 1/2000 (Figures 3E and 5F) or rabbit polyclonal anti-histone H2B antibody (Abcam, Cambridge, U.K.) diluted 1/5000 (Figure 5C). HRP-conjugated goat anti-mouse diluted 1/2000 (GAPDH, Santa Cruz Biotechnology), HRP-conjugated goat anti-rabbit (Erk2, Santa Cruz Biotechnology) diluted 1/2000 and fluorophore-conjugated IRDye 800CW anti-rabbit IgG (Histone H2B, ROCKLAND Immunochemicals) diluted 1/10000 served as secondary antibodies. Detection and quantification of the Western blot shown in Figure 5C was carried out by using the Odyssey infrared imaging system (LI-COR Biosciences, Bad Homburg, Germany).

Northern Blot. Northern blots were performed according to standard procedures as previously described.[25] As specific probes, ~700bp fragments of *WASP*, *GFP* and PRE cDNAs were used to detect RNA transcripts and 18S served as a housekeeping control.

Quantification of Relative RNA Levels. RNA from HT1080ecat or Lin− cells was extracted 5−6 days post-transduction using the RNAzol B (WAK-Chemie Medical GmbH, Steinbach/Ts, Germany) extraction method. Subsequently, RNA was reverse transcribed by QuantiTect Reverse Transcription Kit (Qiagen). cDNA was amplified with Fast SybrGreen reagent (Qiagen) and primers directed against vector specific GFP (5′-CTATAT-CATGGCCGACAAGCAGA-3′ and 5′-GGACTGGGTGCT CAGGTAGTGG-3′), and either murine (QuantiTect Primer Assay MmActb_2_SG, Qiagen) or human beta actin genes (5′-CC TCCCTGGAGAAGAGCTA-3′ and 5′-TCCATGCCCAGGAAG GAAG-3′) on a StepOne Plus light cycler (Applied Biosystems, Carlsbad, CA). Relative RNA quantities were determined by comparative $\Delta\Delta C_T$ method and normalized for copy numbers in transduced cells.

Quantitation of Vector Copy Numbers. Genomic DNA from transduced HT1080ecat and Lin− murine hematopoietic cells was purified with QIAamp DNA Blood Mini and Micro Kits (Qiagen, Hilden, Germany), respectively. Quantitative PCR was performed with Fast SybrGreen reagent (Qiagen) on a StepOnePlus light cycler (Applied Biosystems, Carlsbad, CA) and primers specific for GFP and normalization for input DNA by polypyrimidine tract binding protein 2 amplification (5′-TCT CCATTCCCTATGTTCATGC-3′ and 5′-GTTCCCGCAGAA TGGTGAGGTG-3′). Copy number calculations were performed by the Pfaffl method.[33]

Flow Cytometry and Cell Sorting. Expression of GFP was detected by FACS analysis. Data were collected with a FACSCalibur (BD-Pharmingen, SD, CA) equipped with the standard filter sets. Fluorescence distribution was analyzed using CellQuest software (BD Biosciences, San Jose, CA) and FlowJo (Treestar, Ashland,

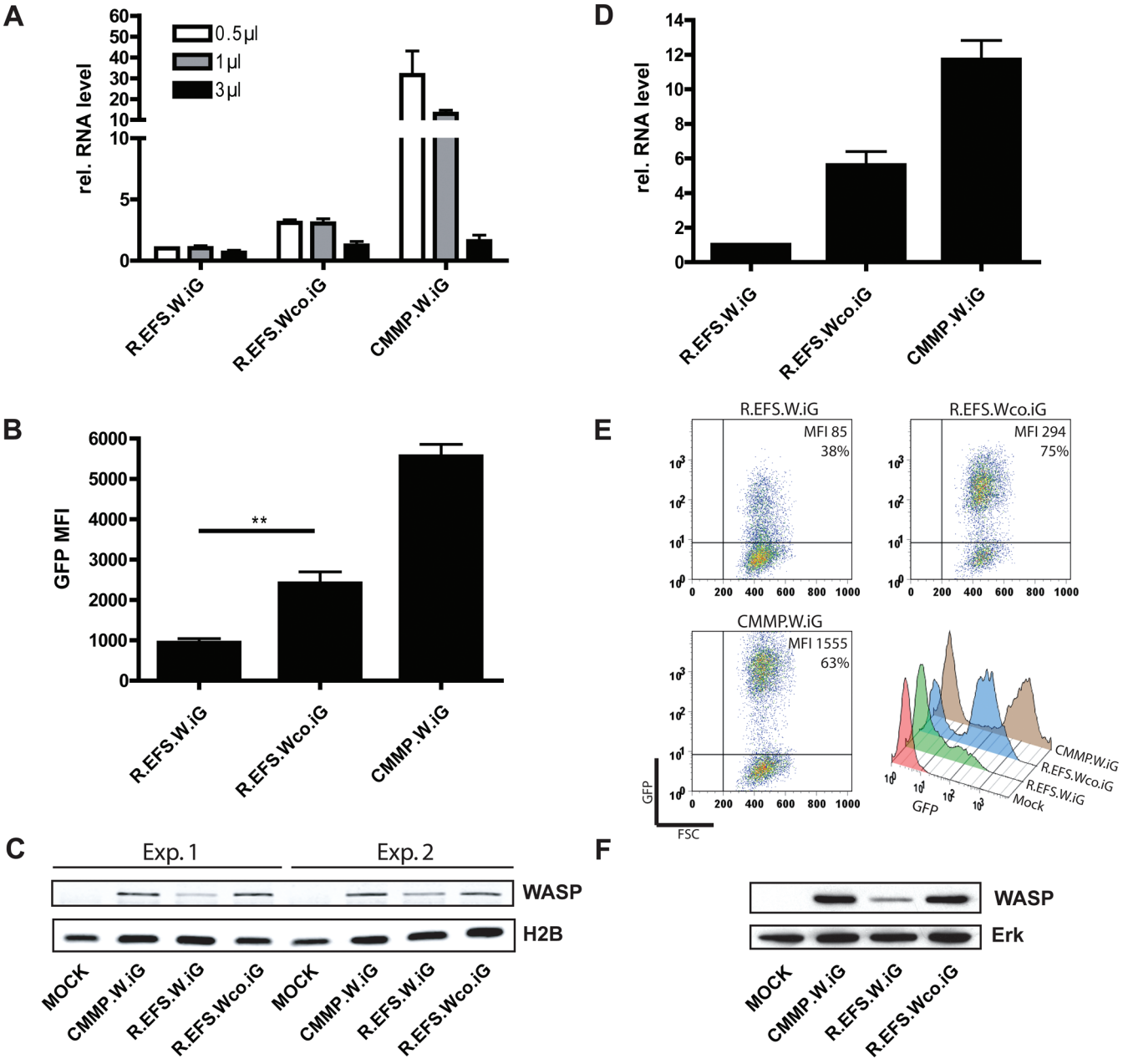

Figure 5. Increase of WAS RNA and protein expression from codon-optimized vectors. (A) HT1080ecat cells were transduced with increasing amounts of three different retroviral vectors expressing either wild-type or codon-optimized (co) WASP from an internal EFS promoter (R.EFS.W.iG or R.EFS.Wco.iG) or wild-type WASP from an LTR driven vector (CMMP.W.iG) in combination with GFP. GFP expression was taken as a surrogate marker for overall vector mediated transcript production and normalized to viral copy number (VCN) in marker positive cells. (B) GFP mean fluorescence intensity of HT1080ecat cells transduced with vectors from A ($n = 3$). (C) Quantitative WASP detection by Western blot in transduced HT1080ecat cells from two representative experiments. Histone H2B served as loading control. Detection of 5 μg of total protein and quantification was performed using the Odyssey infrared imaging system. (D−F) Three wells of murine Lin− negative cells were transduced with vectors from A, and analyzed 5 days post-transduction for GFP expression by flow cytometry, quantitative RT-PCR or Western blot. All wells were identically treated: one harvested for RNA quantification, and the latter two for protein and copy number characterization. (D) Data are shown as relative RNA levels normalized for vector copy numbers in transduced cells. (E) Examplified flow cytometric analysis shown as individual dot plots and in overlay. (F) Corresponding protein levels of cells analyzed in E detected by Western blot using chemiluminescence and 20 μg of total protein. Erk2 served as loading control.

OR, USA). For cell sorting, cells were harvested, washed with PBS and resuspended in PBS supplemented with 10% FCS before being sorted in a FACSAria cell sorter (Cytomation Inc., Fort Collins, CO, USA).

***In Vitro* Differentiation of CD34+ Cells and Magnetic Separation of CD14+ Cells.** Differentiation of CD34+ cells into myeloid progeny was performed as previously described.[24] In brief, eight thousand transduced CD34+ cells were seeded on a monolayer of mitomycin C-treated (10 mg/mL) MS5 feeder cells[34] and incubated for two weeks in IMDM supplemented with 10% human AB serum (Sigma), 5% FCS, 100 U/mL penicillin/streptomycin, 2 mM glutamine, 50 ng/mL hSCF,

20 ng/mL hTPO, 50 ng/mL hFlt3-ligand, 10 ng/mL granulocyte colony-stimulating factor (G-CSF) and 10 ng/mL granulocyte/monocyte colony-stimulating factor (GM-CSF) (CellSystems). To purify CD14+ cells, we used anti-CD14 magnetic beads and separated in an AutoMACS device (Miltenyi Biotech) following the instructions provided by the manufacturer.

Podosome Staining and Detection. Podosomes were detected as described.[24] In brief, 5×10^4 cells were plated on 25 mm^2 coverslips in six-well plates previously coated with 10 mg/mL fibronectin (Roche Diagnostics GmbH) and incubated for 2 h at 37 °C. Cells were fixed for 20 min in 4% para-formaldehyde, permeabilized for 5 min in 0.2% Triton-X-100 in PBS and blocked with 1% BSA for 30 min. Podosomes were stained with anti-vinculin antibody (Sigma, Pool, Dorset, U.K.; dilution 1/50), Cy5-conjugated rabbit anti-mouse IgG F(ab)2 fragment (Jackson ImmunoResearch Europe Ltd., Soham, U.K.; dilution 1/100) and phalloidin-TRITC (Sigma) at 0.1 mg/mL to detect F-actin. Nuclei were labeled with DAPI contained in the mounting solution. Preparations were transferred to slides and examined with a fluorescence microscope Axiovert 200 equipped with an Axioplan 2 imaging system (Carl Zeiss, Göttingen, Germany). Images were captured with a PLAN-APOCHROMAT 63×/1.4 oil objective and acquired with the Openlab 3.1.7 imaging software (Improvision Ltd., Coventry, U.K.). Percentage of cells displaying podosomes was counted by enumerating at least 200 cells per sample.

RESULTS

Development of Self-Inactivating Vectors To Substitute for the Clinically Used LTR-Driven Gammaretroviral Vector. We designed a series of novel gammaretro- and lentiviral vectors with self-inactivating (SIN) configuration, which ensures a decreased risk of activating cellular proto-oncogenes, for the expression of WASP (Figure 1). In addition to the constructed gammaretroviral SIN vectors (R) as well as lentiviral SIN vectors (L), we also included the clinically used LTR-driven gammaretroviral vector (CMMP) for comparison. In the SIN vectors, the expression of the therapeutic transgene (either wild-type or codon optimized for optimal expression in human cells) and the marker gene (GFP) is driven by the EFS (EF1-α short) and the SFFV (spleen focus forming virus U3) internal promoters, respectively. All vectors were developed with a split packaging design to minimize the risk of RCR (replication competent retrovirus) formation and to gain maximum space for the insertion of transgene cassettes. Titers of both SIN-gammaretro- and SIN-lentiviral vector supernatants did not significantly differ from those obtained with the gammaretroviral vector with intact LTR that is currently being used in the Hannover clinical trial.[11] Importantly, the replacement of the wild-type *WASP* cDNA (W) with the novel codon optimized sequence (Wco) led to equally high titers as the vectors carrying the wild-type cDNA (in the range of 5 × 10e7 − 1.5 × 10e8 tu/ml) (Figure 2).

A SIN-Gammaretroviral Vector with a Weak Cellular Promoter and a Codon-Optimized WASP cDNA with Improved WASP Expression. Next, we evaluated the feasibility of the novel codon-optimized WASP (Wco) sequence to improve the RNA expression. A comparative Northern blot analysis of HT1080ecat cells transduced with SIN-retroviral vectors (Figure 3A) revealed that Wco clearly improved RNA expression, thus allowing the use of a weaker cellular promoter (EFS) to reach the same protein levels. The combination of the more physiological cellular promoter, EFS, and the new transgene, Wco, yielded nearly the same RNA levels as the strong promoter of viral origin, SFFV, and the wild-type cDNA (wt) (Figure 3C). SIN-lentiviral vectors were shown to have similar expression levels compared to their gammaretroviral counterparts (Figures 3B and 3D), even in the absence of marker gene, in samples with very low number of viral integrations (≤0.9 copies per genome), as it is desired in a clinical scenario. Noteworthy, the SIN design of our retroviral vectors prevented the transcription of unspliced full-length retroviral RNA harboring the packaging signal ψ (see Figure 3A, full length RNA would be expected between 5000 and 6000 bp), which improves the safety of these vectors.

To further characterize transgene expression, an immunoblot was performed to specifically detect the expression of WASP upon transduction with the new vectors, where we compared samples with similarly low number of viral integrations (Figure 3E). The substitution of the W (wild-type WASP) by the Wco cDNA resulted in higher protein expression, a finding consistent with the phenomenon observed at the RNA level. As before, it was the combination of EFS and Wco that yielded the same levels of protein expression than the LTR-driven gammaretroviral CMMP vector used in the Hannover clinical trial.

Efficient Transgene Expression in Murine Wasp ko Hematopoietic Precursor Cells. To comparatively assess the efficiency of our vector R.EFS.Wco.iG in hematopoietic target cells for gene therapy in the murine model, Wasp ko Lin− cells were transduced with SIN-gammaretro- and SIN-lentiviral vectors containing Wco with multiplicities of infection (MOI) of 1, 3, and 5, respectively. Four days after transduction, samples were analyzed by flow cytometry. As expected, we were able to effectively transduce Wasp ko Lin− cells even at low MOIs with all tested vectors. Increasing the vector dose resulted in higher transduction rates in all cases (Figure 4A). Transgene expression driven by the cellular EFS promoter was lower than the expression by the viral SFFV promoter (Figure 4B; *Y*-axis: GFP mean fluorescence intensity) and transduction rates achieved with both promoters were very similar. SIN-gammaretroviral vectors were slightly more efficient than their lentiviral counterparts (Figure 4A,C). This might be attributable to the differences in integration site preferences. These results show that these novel vectors, R.EFS.Wco.iG and L.EFS.Wco.iG, can efficiently transduce murine hematopoietic precursor cells. The EFS-driven vectors were only 2(−3)-fold weaker in terms of fluorescent intensities compared to their counterparts with the strong internal SFFV promoter.

The EFS-Driven SIN Vector with Codon-Optimized *WASP* cDNA Achieves Similar WAS Protein Expression Levels Compared to the Clinically Used CMMP Vector. Encouraged by the preceding results, we were interested to measure more precisely the extent of improvement of RNA and protein expression for a smaller set of promising vectors. Therefore, we chose the gammaretroviral SIN vector (R.EFS.W.iG and its codon-optimized counterpart R.EFS.Wco.iG) and compared it to the LTR-driven gammaretroviral vector CMMP.W.iG, a derivative of the clinical WASP vector. With these vectors, we transduced human HT1080ecat cells with 3 different amounts of concentrated viral supernatants (0.5, 1, 3 μL) using comparable MOIs and harvested the cells after 6 days for RNA isolation, FACS analysis and Western blot analysis (Figure 5A−C). Cellular RNA was reverse transcribed and quantified in relation to a housekeeping gene. The resulting RNA values were displayed as relative RNA quantity and were normalized for viral copy number and transduction rates. The R.EFS.Wco.iG expressed

3-fold more RNA, the CMMP.W.iG even 22-fold more RNA than the basic R.EFS.W.iG vector (Figure 5A). Of note, only values derived from cells transduced with 0.5 and 1 μL of supernatant were used for quantification since overexpression of WASP seems to be toxic as indicated by reduced WASP expression over time (data not shown). As determined by FACS analysis, EGFP protein expression for R.EFS.Wco.iG was 2.5-fold higher and for the CMMP.W.iG vector 5.5-fold higher in comparison to the R.EFS.W.iG vector (Figure 5B). Interestingly, when determining WAS protein expression levels by Western blot these differences were less pronounced (2 different representative experiments shown, 4 individual measurements performed per vector for quantification). Here the R.EFS.Wco.iG performed very similarly in relation to the CMMP.W.iG vector and enhanced protein expression 2.2-fold (CMMP.W.iG 2.1-fold better than R.EFS.W.iG) in comparison to R.EFS.W.iG (Figure 5C), as determined by Odyssey infrared imaging system for protein quantification. This shows that the new codon-optimized R.EFS.Wco.iG vector performs equally well as the clinical CMMP vector in terms of WAS protein expression. Although the CMMP.W.iG vector shows higher RNA levels and GFP protein levels, this was not observed for WAS protein expression, probably due to the suboptimal Kozak sequence actgccATGa in front of the WAS ORF in the CMMP vector.

Next, we were interested to transfer our observation to Wasp ko Lin− bone marrow cells. For R.EFS.Wco.iG and CMMP.W.iG we observed a 5-fold and 12-fold higher RNA-expression, compared to R.EFS.W.iG (Figure 5D), again normalized for transduction efficiency and copy number. Analyzing GFP expression via FACS we found as expected higher mean fluorescence intensity for R.EFS.Wco.iG, which were highest for CMMP.W.iG (Figure 5E). However, again, the WAS protein levels of R.EFS.Wco.iG and CMMP.W.iG were again very similar and approximately 2-fold higher than R.EFS.W.iG (Figure 5F). This demonstrates that the codon-optimized R.EFS.Wco.iG, while being safety-optimized, shows comparable expression to the clinical vector CMMP.W.iG in Wasp ko lineage negative bone marrow cells.

To determine the WAS protein expression profile in Wasp ko bone marrow derived cells, we performed immunofluorescence microscopy analysis and monitored GFP and WAS protein expression as well as F-actin expression. Hoechst staining was included to mark the nuclear compartment. In all transduced ko BM cells, we could observe clear WAS protein expression, resembling the typical granular cytoplasmic staining of WASP, very similar to the presented picture in wild-type BM cells (Figure 6). Based on these data, we performed 3D reconstructions of transduced Wasp ko bone marrow derived cells (Supplementary Movies 1−5 in the Supporting Information).

In summary, the new R.EFS.Wco.iG vector shows very similar WAS protein levels compared to the clinical CMMP.W.iG vector, for which clinical efficacy has already been obtained.

An EFS-Driven SIN Vector Corrects the WAS Phenotype in Patient-Derived Human Hematopoietic Cells. After demonstrating that the newly generated vector, R.EFS.Wco.iG, allows for higher RNA levels and improved transgene expression, we wanted to further evaluate whether it also provides, in a clinically more relevant scenario, the same efficiency and functionality as the earlier vector used in the clinical trial in Hannover. To this aim, we tested whether this vector could reconstitute the WAS phenotype in CD34+ derived WASP-deficient monocytes. WASP-deficient macrophages and dendritic cells are characterized by the abscense of adhesion structures called podosomes,[27] a hallmark of the disease. To assess the functionality of the protein expressed by Wco, we investigated whether retroviral gene transfer into WASP-deficient CD34+ cells could reconstitute the formation of podosomes in myeloid cells differentiated *in vitro*. CD34+ cells from two independent patients, WAS1 and WAS2, were transduced either with CMMP.W.iG or R.EFS.Wco.iG at an MOI of 5. Three days later, the cells were differentiated into myeloid progeny (see Materials and Methods for details). Subsequently, CD14+ cells were magnetically separated and stained for vinculin and F-actin intracellularly. The specific colocalization of vinculin and F-actin corresponds to the organized structure of podosomes.

The transduction of CD34+ cells from patient WAS1 with R.EFS.Wco.iG and CMMP resulted in 16.5% and 12.3% GFP+ cells, respectively. After subsequent myeloid differentiation, the percentage of CD14+ GFP+ cells was 19.5% with R.EFS.Wco.iG and 27.2% with CMMP (Figure 7A). Podosomes were detected in 23% and 28% of CD14+ cells transduced with our novel vector and with CMMP, respectively (Figure 7B,C).

The transduction of CD34+ cells from patient WAS2 with R.EFS.Wco. iG and CMMP resulted in 15.2% and 7.5% GFP+ cells, respectively. After subsequent myeloid differentiation, the percentage of CD14+ GFP+ cells was 13.3% with R.EFS.Wco.iG and 15.6% with CMMP (Figure 7A). Podosomes were detected in 30% and 37% of CD14+ cells transduced with our novel vector and with CMMP, respectively (Figure 7B,C).

As expected, *in vitro* differentiated WASP-deficient CD14+ cells completely failed to assemble vinculin and F-actin to form podosomes in both patients, whereas two independent healthy individual donors displayed 63% and 77% CD14+ cells with podosomes, respectively (Figure 7B,C).

These findings are consistent with previous results obtained in immortalized B cells from two other independent WAS patients, named WAS3 and WAS4 (Supplementary Figure 1 in the Supporting Information), where the reconstitution of WASP expression upon transduction with R.EFS.W.iG was very similar to that obtained with the CMMP vector.

Taken together, these data show that the SIN-gammaretroviral vector, containing a novel codon optimized version of *WASP* cDNA driven by an internal promoter of cellular origin, can transduce the target cell population for gene therapy as efficiently as the clinically used vector. Importantly, the protein expressed by Wco is functional and allows for efficient reconstitution of the aberrant cytoskeleton of the myeloid progeny of WASP deficient CD34+ cells.

DISCUSSION

The clinical trial for WAS that is currently ongoing at the Hannover Medical School (Germany) has recently reported the successful correction of all blood cell lineages in the first two treated patients, including for the first time correction of autoimmunity and platelet numbers after transplantation of retroviral vector-transduced HSC in patients.[11] Noteworthy, the fractions of corrected lymphocytes increased over time, and both patients have markedly improved their clinical condition with respect to the susceptibility to infection, autoimmunity, and bleeding. These findings could be confirmed in additional patients treated with the conventional LTR-driven gammaretroviral vector CMMP in Hannover (privileged communication, C. Klein). This clinical trial provides first proof-of-principle that gene therapy for WAS is feasible with a follow-up of up to 4.5 years after gene

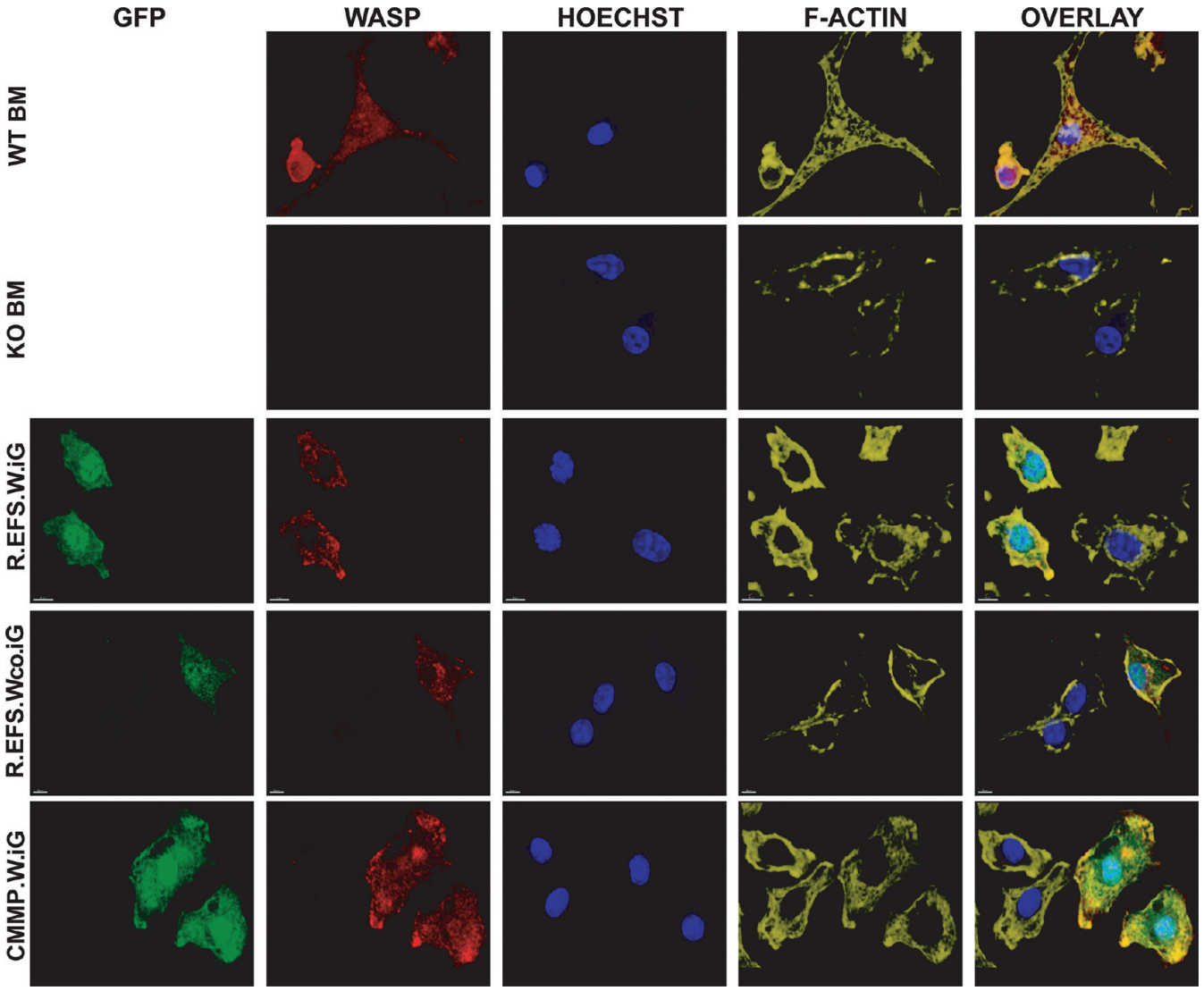

Figure 6. Retroviral transduction of murine Wasp ko bone marrow cells reconstitutes WASP expression. The figure shows representative bone marrow derived adherent cells grown on glass coverslips and stained for WASP (red), DNA (blue; Hoechst 33342) and F-actin (yellow) via intracellular immunofluorescence staining. Microscope settings were adjusted such that in Wasp ko cells no cytoplasmic signal could be detected. GFP+ cells transduced either with R.EFS.W.iG, R.EFS.Wco.iG or CMMP.W.iG show the typical granular cytoplasmic staining of WASP, similar to wild-type cells. The protein expression level in the investigated transduced cells approximately matches the level observed in wild-type cells.

therapy, indicating that early hematopoietic progenitor/stem cells contributing quantitatively to all cell lineages of blood were successfully corrected.[11] However, an extensive study of the clonal inventory of the first treated patients revealed that *LMO2*, *CCND2*, and *MDS1/EVI1*, were, among others, preferentially prevalent.[11] The activation of these proto-oncogenes can potentially cause severe side effects as seen in previous similar clinical trials.[12,14] Although no persistent clonal imbalance has been observed so far in the first two treated WAS patients, the risk of insertional mutagenesis remains a drawback as evidenced by a recent leukemia case observed in one patient treated in this series[35,36] (C. Klein, unpublished). Taken together, the WAS and SCID trials clearly show efficacy but also demonstrate the well-recognized insertional gene activation potential of first generation LTR-driven gammaretroviral vectors.[35]

In this study, we present a novel vector for the gene therapy of WAS that combines improved safety features and similar efficacy as the clinically used vector. The risk of activating cellular proto-oncogenes has been significantly reduced by using a SIN-design[15,17] and the EFS promoter, which is much less likely to activate neighboring genes compared to strong viral promoters.[16,37] Gammaretroviral SIN vectors with cellular promoters have been successfully used to correct the phenotype of X-linked severe combined immunodeficiency[18] and could reduce the manifestations of mucopolysaccharidosis type I in mice.[38] A comparative test of several cellular promoters (EFS, PGK, and WASP; data not shown) showed that EFS yielded the highest MFI values and was hence selected here.

In an international consortial initiative, laboratories in Milano, London and Paris successfully used a lentiviral SIN vector harboring the natural 1.6 kb WASP promoter driving the wild-type WASP cDNA and could correct the phenotype in a *Wasp* ko mouse model.[39−41] Recently, a clinical trial with this WASP-promotor driven vector construct was initiated.

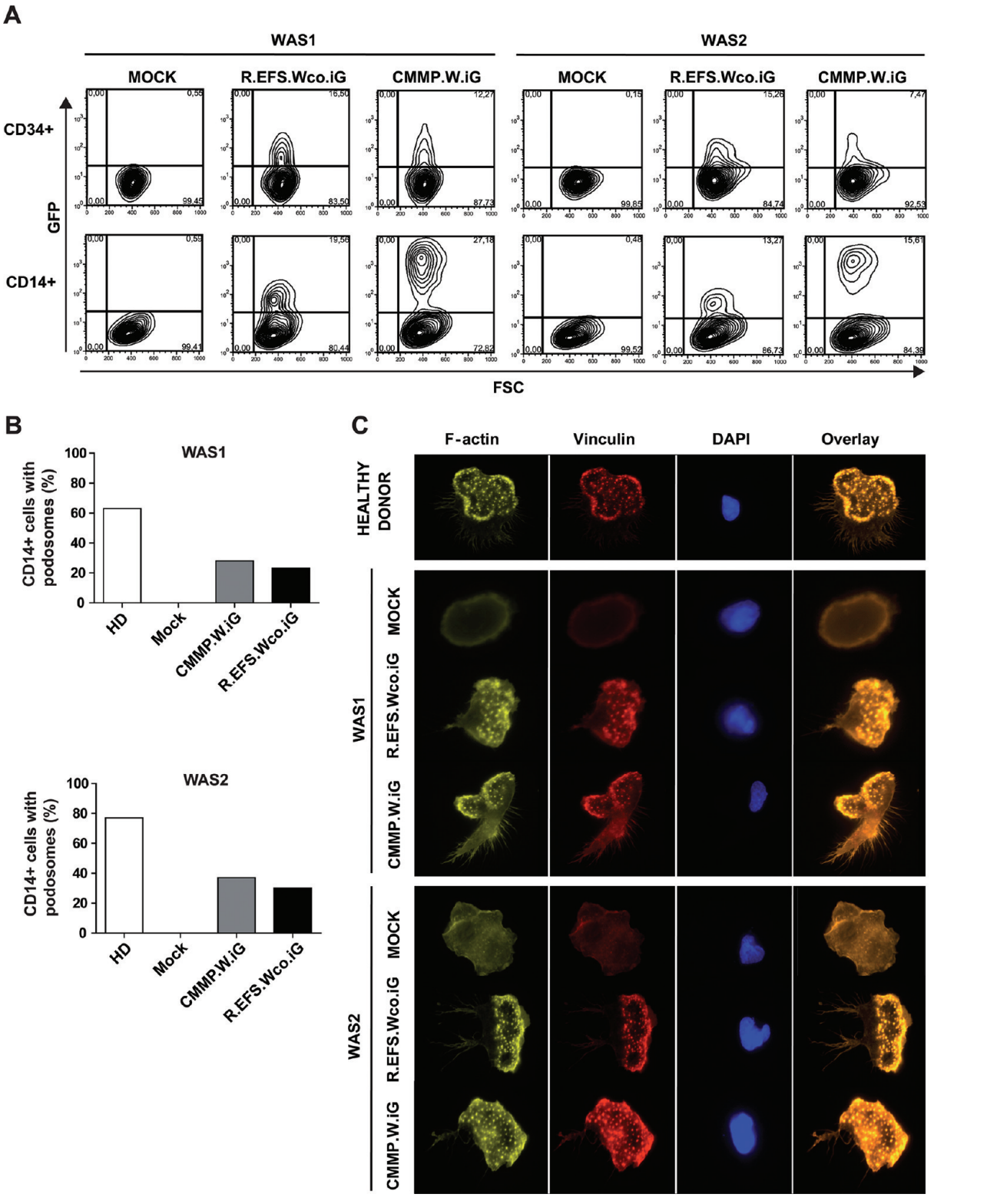

Figure 7. Functional restoration of podosome formation after gene transfer. CD34+ cells from patients WAS1 and WAS2 were transduced either with CMMP.W.iG or with R.EFS.Wco.iG at an MOI = 5 and differentiated into myeloid cells. Podosomes correspond to a specific colocalization of vinculin (red) and actin (green). Cell nuclei are recognized by DAPI stain (blue). Mock transduced cells express vinculin and actin but fail to coassemble them into organized structures. (A) FACS analysis for detection of GFP in transduced CD34+ cells (upper panel) and differentiated CD14+ cells (bottom panel). Numbers in the upper right quadrant indicate the percentage of GFP positive cells. (B) Percentage of CD14+ cells with podosomes in an untransduced healthy donor (HD) and in transduced and untransduced WAS1 and WAS2 patients. (C) Representative stainings of untransduced healthy donor cells (top panel), reconstituted cells from WAS1 (middle panel) and transduced cells from WAS2 (bottom panel), both compared to untreated patient cells.

Here, we chose a gammaretroviral vector as the current clinical trial in Hannover has established gammaretroviral transduction conditions that are of sufficient potency for long-term disease correction. Furthermore, when the vector cassette does not contain strong enhancer elements, the gammaretroviral integration pattern could be advantageous as it may be less likely than the lentiviral to cause disruptions of cellular genes. Since *ex vivo* gene therapy targets hematopoietic cells, we considered that a hematopoiesis-specific promoter is not needed. We thus used the extensively safety-evaluated EF1-α short promoter[16,42] driving a codon-optimized *WASP* cDNA. The wild-type *WASP* cDNA sequence was altered to optimal human codon usage for translation into protein, destabilizing *cis*-acting sequences, RNA secondary structures and possible splice sites were removed (see also Supplementary Figure 2 in the Supporting Information providing a sequence alignment), and two STOP codons were added to ensure efficient termination. These modifications resulted in higher gene expression with all vectors in all cell types tested, probably reflecting the improved processivity of *WASPco*. Importantly, in the *WASP* coding sequence (encoding the GRSGPLPPXPP motifs and poly-proline motifs; compare Supplementary Figures 2 and 3 in the Supporting Information), a number of repetitive sequences were observed. We took advantage of the codon bias and wobbled the DNA to remove these elements and to prevent hot spots for jumps of reverse transcriptase. Similarly, codon-optimization could enhance transgene expression in other clinically relevant settings (e.g., CGD).[43−45] Using a codon-optimization strategy, we can achieve good expression levels on RNA and protein level (see Figures 3 and 5) despite using a moderately expressing internal promoter (such as the cellular promoter EF1-α short, EFS). Importantly, we were able to reach a WAS protein expression level similar to the clinically used LTR-driven CMMP vector. To assess vector performance in a more clinically relevant setting, we transduced murine Wasp ko HSPC, the target cell population for bone marrow transplantation in preclinical models, and also human CD34+ hematopoietic cells. When testing the gammaretroviral SIN vector R.EFS.Wco.iG in CD34+ cells from WAS patients, transduction rates obtained did not differ significantly from those with the clinically used gammaretroviral LTR-driven CMMP vector. The myeloid progeny of CD 34+ cells treated with R.EFS.Wco.iG displayed a similar morphology and phenotypical correction compared to those treated with the CMMP vector and were indistinguishable from the healthy donor. These results demonstrate, in primary patient cells, that our novel vector can correct the aberrant cytoskeleton (Figure 7), providing sufficient *WASP* expression to rescue the formation of podosomes as efficiently as the vector currently used in the clinical trial, despite the low MOI. Interestingly, it was previously shown that WASP levels exceeding 60% of normal protein expression were required to restore podosome formation and physiological cytoskeleton-dependent activities,[46] thus implying that WASP protein levels from our vector are fairly high and in the "physiological" range. The present data validate the ability to restore WASP expression in patients' CD34+ cells while preserving their *in vitro* differentiation potential, two important requisites for clinical use.

This study also shows that this new safety-modified vector can be produced at high titers in human 293T cells, within the range necessary for clinical applications, as determined for several pseudotypes (VSVg, GALV, and ecotropic). Of note, our gammaretroviral vector backbone is devoid of viral gene remnants and devoid of any overlap between vector and helper plasmids,[47] reducing the likelihood of formation of replication competent retroviruses and potentially immunogenic expression of viral proteins from transduced cells.

For these reasons, the new SIN vectors (e.g., R.EFS.Wco or its equally well expressing lentiviral counterpart) with the cellular EFS promoter and codon-optimized WASP appear to be reasonable candidates for potential use in a safer second generation gene therapy protocol for WAS, with decreased risk of insertional mutagenesis.

■ ASSOCIATED CONTENT

Supporting Information. Figures depicting reconstitution of WASP expression in WASP-deficient B cells, alignment of wild-type *WASP* vs codon-optimized *WASP* cDNA, and alignment of protein coding sequence of WASP vs codon-optimized WASP proteins. Movies of 3D reconstruction of WAS protein expression in wild-type BM cells, 3D reconstruction of Wasp ko BM cells, 3D reconstruction of Wasp ko BM cells transduced with R.EFS.W.iG vector, 3D reconstruction of Wasp ko BM cells transduced with R.EFS.Wco.iG, and 3D reconstruction of Wasp ko BM cells transduced with CMMP.W.iG. This material is available free of charge via the Internet at http://pubs.acs.org.

■ AUTHOR INFORMATION

Corresponding Authors

*C.K.: Department of Pediatrics, Dr von Hauner'sches Kinderspital, University Children's Hospital, Lindwurmstrasse 4, D-80337 Munich, Germany; e-mail, christoph.klein@med.uni-muenchen.de; phone, +49-89-5160-7700; fax, +49-89-5160-7702. A.S.: Institute of Experimental Hematology, Hannover Medical School, Carl-Neuberg-Straße 1, D-30625 Hannover, Germany; e-mail, schambach.axel@mh-hannover.de; phone, +49-511-532-5139; fax, +49-511-532-5105.

Present Addresses

§Laboratorio de Terapia Génica y Células Madre, Instituto Tecnológico de Chascomús (IIB-INTECH), Camino de Circunvalación Laguna km 6, B7130IWA, Chascomús, Argentina.

■ ACKNOWLEDGMENT

This work was supported by grants from German Ministry for Research and Education (iGene, PidNet, IFB-Tx (01EO0802), the German Academic Exchange Service (DAAD (0315187)), the Deutsche Forschungsgemeinschaft (SPP1230 and Cluster of Excellence REBIRTH (EXC 62/1) and the European Union (Integrated Project CELL-PID). We would like to thank Jana Diestelhorst, Girmay Asgedom, Sabine Knoess, Johanna Krause and Diana Knetsch for technical assistance. We are grateful to Dr. Ballmeier and the cell sorter sorter facility at MHH for assistance with cell sorting, and to Dr. Rudi Bauerfeind and the confocal microscopy facility for assistance with confocal imaging. The authors disclose any financial interest in association with the submitted material.

■ REFERENCES

(1) Ochs, H. D.; Thrasher, A. J. The Wiskott-Aldrich syndrome. *J. Allergy Clin. Immunol.* **2006**, *117* (4), 725−38; quiz 739.

(2) Derry, J. M.; Ochs, H. D.; Francke, U. Isolation of a novel gene mutated in Wiskott-Aldrich syndrome. *Cell* **1994**, *78* (4), 635–44.

(3) Burns, S.; Cory, G. O.; Vainchenker, W.; Thrasher, A. J. Mechanisms of WASp-mediated hematologic and immunologic disease. *Blood* **2004**, *104* (12), 3454–62.

(4) Sullivan, K. E.; Mullen, C. A.; Blaese, R. M.; Winkelstein, J. A. A multiinstitutional survey of the Wiskott-Aldrich syndrome. *J. Pediatr.* **1994**, *125* (6 Part 1), 876–85.

(5) Cavazzana-Calvo, M.; Hacein-Bey, S.; de Saint Basile, G.; Gross, F.; Yvon, E.; Nusbaum, P.; Selz, F.; Hue, C.; Certain, S.; Casanova, J. L.; Bousso, P.; Deist, F. L.; Fischer, A. Gene therapy of human severe combined immunodeficiency (SCID)-X1 disease. *Science* **2000**, *288* (5466), 669–72.

(6) Ozsahin, H.; Le Deist, F.; Benkerrou, M.; Cavazzana-Calvo, M.; Gomez, L.; Griscelli, C.; Blanche, S.; Fischer, A. Bone marrow transplantation in 26 patients with Wiskott-Aldrich syndrome from a single center. *J. Pediatr.* **1996**, *129* (2), 238–44.

(7) Filipovich, A. H.; Stone, J. V.; Tomany, S. C.; Ireland, M.; Kollman, C.; Pelz, C. J.; Casper, J. T.; Cowan, M. J.; Edwards, J. R.; Fasth, A.; Gale, R. P.; Junker, A.; Kamani, N. R.; Loechelt, B. J.; Pietryga, D. W.; Ringden, O.; Vowels, M.; Hegland, J.; Williams, A. V.; Klein, J. P.; Sobocinski, K. A.; Rowlings, P. A.; Horowitz, M. M. Impact of donor type on outcome of bone marrow transplantation for Wiskott-Aldrich syndrome: collaborative study of the International Bone Marrow Transplant Registry and the National Marrow Donor Program. *Blood* **2001**, *97* (6), 1598–603.

(8) Anderson, W. F. Prospects for human gene therapy. *Science* **1984**, *226* (4673), 401–9.

(9) Aiuti, A.; Slavin, S.; Aker, M.; Ficara, F.; Deola, S.; Mortellaro, A.; Morecki, S.; Andolfi, G.; Tabucchi, A.; Carlucci, F.; Marinello, E.; Cattaneo, F.; Vai, S.; Servida, P.; Miniero, R.; Roncarolo, M. G.; Bordignon, C. Correction of ADA-SCID by stem cell gene therapy combined with nonmyeloablative conditioning. *Science* **2002**, *296* (5577), 2410–3.

(10) Ott, M. G.; Schmidt, M.; Schwarzwaelder, K.; Stein, S.; Siler, U.; Koehl, U.; Glimm, H.; Kuhlcke, K.; Schilz, A.; Kunkel, H.; Naundorf, S.; Brinkmann, A.; Deichmann, A.; Fischer, M.; Ball, C.; Pilz, I.; Dunbar, C.; Du, Y.; Jenkins, N. A.; Copeland, N. G.; Luthi, U.; Hassan, M.; Thrasher, A. J.; Hoelzer, D.; von Kalle, C.; Seger, R.; Grez, M. Correction of X-linked chronic granulomatous disease by gene therapy, augmented by insertional activation of MDS1-EVI1, PRDM16 or SETBP1. *Nat. Med.* **2006**, *12* (4), 401–9.

(11) Boztug, K.; Schmidt, M.; Schwarzer, A.; Banerjee, P. P.; Diez, I. A.; Dewey, R. A.; Bohm, M.; Nowrouzi, A.; Ball, C. R.; Glimm, H.; Naundorf, S.; Kuhlcke, K.; Blasczyk, R.; Kondratenko, I.; Marodi, L.; Orange, J. S.; von Kalle, C.; Klein, C. Stem-cell gene therapy for the Wiskott-Aldrich syndrome. *N. Engl. J. Med.* **2010**, *363* (20), 1918–27.

(12) Howe, S. J.; Mansour, M. R.; Schwarzwaelder, K.; Bartholomae, C.; Hubank, M.; Kempski, H.; Brugman, M. H.; Pike-Overzet, K.; Chatters, S. J.; de Ridder, D.; Gilmour, K. C.; Adams, S.; Thornhill, S. I.; Parsley, K. L.; Staal, F. J.; Gale, R. E.; Linch, D. C.; Bayford, J.; Brown, L.; Quaye, M.; Kinnon, C.; Ancliff, P.; Webb, D. K.; Schmidt, M.; von Kalle, C.; Gaspar, H. B.; Thrasher, A. J. Insertional mutagenesis combined with acquired somatic mutations causes leukemogenesis following gene therapy of SCID-X1 patients. *J. Clin. Invest.* **2008**, *118* (9), 3143–50.

(13) Hacein-Bey-Abina, S.; Garrigue, A.; Wang, G. P.; Soulier, J.; Lim, A.; Morillon, E.; Clappier, E.; Caccavelli, L.; Delabesse, E.; Beldjord, K.; Asnafi, V.; MacIntyre, E.; Dal Cortivo, L.; Radford, I.; Brousse, N.; Sigaux, F.; Moshous, D.; Hauer, J.; Borkhardt, A.; Belohradsky, B. H.; Wintergerst, U.; Velez, M. C.; Leiva, L.; Sorensen, R.; Wulffraat, N.; Blanche, S.; Bushman, F. D.; Fischer, A.; Cavazzana-Calvo, M. Insertional oncogenesis in 4 patients after retrovirus-mediated gene therapy of SCID-X1. *J. Clin. Invest.* **2008**, *118* (9), 3132–42.

(14) Stein, S.; Ott, M. G.; Schultze-Strasser, S.; Jauch, A.; Burwinkel, B.; Kinner, A.; Schmidt, M.; Kramer, A.; Schwable, J.; Glimm, H.; Koehl, U.; Preiss, C.; Ball, C.; Martin, H.; Gohring, G.; Schwarzwaelder, K.; Hofmann, W. K.; Karakaya, K.; Tchatchou, S.; Yang, R.; Reinecke, P.; Kuhlcke, K.; Schlegelberger, B.; Thrasher, A. J.; Hoelzer, D.; Seger, R.; von Kalle, C.; Grez, M. Genomic instability and myelodysplasia with monosomy 7 consequent to EVI1 activation after gene therapy for chronic granulomatous disease. *Nat. Med.* **2010**, *16* (2), 198–204.

(15) Modlich, U.; Bohne, J.; Schmidt, M.; von Kalle, C.; Knoss, S.; Schambach, A.; Baum, C. Cell-culture assays reveal the importance of retroviral vector design for insertional genotoxicity. *Blood* **2006**, *108* (8), 2545–53.

(16) Zychlinski, D.; Schambach, A.; Modlich, U.; Maetzig, T.; Meyer, J.; Grassman, E.; Mishra, A.; Baum, C. Physiological promoters reduce the genotoxic risk of integrating gene vectors. *Mol. Ther.* **2008**, *16* (4), 718–25.

(17) Montini, E.; Cesana, D.; Schmidt, M.; Sanvito, F.; Bartholomae, C. C.; Ranzani, M.; Benedicenti, F.; Sergi, L. S.; Ambrosi, A.; Ponzoni, M.; Doglioni, C.; Di Serio, C.; von Kalle, C.; Naldini, L. The genotoxic potential of retroviral vectors is strongly modulated by vector design and integration site selection in a mouse model of HSC gene therapy. *J. Clin. Invest.* **2009**, *119* (4), 964–75.

(18) Thornhill, S. I.; Schambach, A.; Howe, S. J.; Ulaganathan, M.; Grassman, E.; Williams, D.; Schiedlmeier, B.; Sebire, N. J.; Gaspar, H. B.; Kinnon, C.; Baum, C.; Thrasher, A. J. Self-inactivating gammaretroviral vectors for gene therapy of X-linked severe combined immunodeficiency. *Mol. Ther.* **2008**, *16* (3), 590–8.

(19) Charrier, S.; Dupre, L.; Scaramuzza, S.; Jeanson-Leh, L.; Blundell, M. P.; Danos, O.; Cattaneo, F.; Aiuti, A.; Eckenberg, R.; Thrasher, A. J.; Roncarolo, M. G.; Galy, A. Lentiviral vectors targeting WASp expression to hematopoietic cells, efficiently transduce and correct cells from WAS patients. *Gene Ther.* **2007**, *14* (5), 415–28.

(20) Hematti, P.; Hong, B. K.; Ferguson, C.; Adler, R.; Hanawa, H.; Sellers, S.; Holt, I. E.; Eckfeldt, C. E.; Sharma, Y.; Schmidt, M.; von Kalle, C.; Persons, D. A.; Billings, E. M.; Verfaillie, C. M.; Nienhuis, A. W.; Wolfsberg, T. G.; Dunbar, C. E.; Calmels, B. Distinct Genomic Integration of MLV and SIV Vectors in Primate Hematopoietic Stem and Progenitor Cells. *PLoS Biol.* **2004**, *2* (12), e423.

(21) Schroder, A. R.; Shinn, P.; Chen, H.; Berry, C.; Ecker, J. R.; Bushman, F. HIV-1 integration in the human genome favors active genes and local hotspots. *Cell* **2002**, *110* (4), 521–9.

(22) Modlich, U.; Baum, C. Preventing and exploiting the oncogenic potential of integrating gene vectors. *J. Clin. Invest.* **2009**, *119* (4), 755–8.

(23) Maruggi, G.; Porcellini, S.; Facchini, G.; Perna, S. K.; Cattoglio, C.; Sartori, D.; Ambrosi, A.; Schambach, A.; Baum, C.; Bonini, C.; Bovolenta, C.; Mavilio, F.; Recchia, A. Transcriptional enhancers induce insertional gene deregulation independently from the vector type and design. *Mol. Ther.* **2009**, *17* (5), 851–6.

(24) Dewey, R. A.; Avedillo Diez, I.; Ballmaier, M.; Filipovich, A.; Greil, J.; Gungor, T.; Happel, C.; Maschan, A.; Noyan, F.; Pannicke, U.; Schwarz, K.; Snapper, S.; Welte, K.; Klein, C. Retroviral WASP gene transfer into human hematopoietic stem cells reconstitutes the actin cytoskeleton in myeloid progeny cells differentiated in vitro. *Exp. Hematol.* **2006**, *34* (9), 1161–9.

(25) Schambach, A.; Bohne, J.; Chandra, S.; Will, E.; Margison, G. P.; Williams, D. A.; Baum, C. Equal potency of gammaretroviral and lentiviral SIN vectors for expression of O6-methylguanine-DNA methyltransferase in hematopoietic cells. *Mol. Ther.* **2006**, *13* (2), 391–400.

(26) Modlich, U.; Navarro, S.; Zychlinski, D.; Maetzig, T.; Knoess, S.; Brugman, M. H.; Schambach, A.; Charrier, S.; Galy, A.; Thrasher, A. J.; Bueren, J.; Baum, C. Insertional transformation of hematopoietic cells by self-inactivating lentiviral and gammaretroviral vectors. *Mol. Ther.* **2009**, *17* (11), 1919–28.

(27) Linder, S.; Nelson, D.; Weiss, M.; Aepfelbacher, M. Wiskott-Aldrich syndrome protein regulates podosomes in primary human macrophages. *Proc. Natl. Acad. Sci. U.S.A.* **1999**, *96* (17), 9648–53.

(28) Schambach, A.; Mueller, D.; Galla, M.; Verstegen, M. M.; Wagemaker, G.; Loew, R.; Baum, C.; Bohne, J. Overcoming promoter competition in packaging cells improves production of self-inactivating retroviral vectors. *Gene Ther.* **2006**, *13* (21), 1524–33.

(29) Dull, T.; Zufferey, R.; Kelly, M.; Mandel, R. J.; Nguyen, M.; Trono, D.; Naldini, L. A third-generation lentivirus vector with a conditional packaging system. *J. Virol.* **1998**, *72* (11), 8463–71.

(30) Maetzig, T.; Brugman, M. H.; Bartels, S.; Heinz, N.; Kustikova, O. S.; Modlich, U.; Li, Z.; Galla, M.; Schiedlmeier, B.; Schambach, A.; Baum, C. Polyclonal fluctuation of lentiviral vector-transduced and expanded murine hematopoietic stem cells. *Blood* **2011**, *117*, 3053–64.

(31) Schambach, A.; Bohne, J.; Baum, C.; Hermann, F. G.; Egerer, L.; von Laer, D.; Giroglou, T. Woodchuck hepatitis virus post-transcriptional regulatory element deleted from X protein and promoter sequences enhances retroviral vector titer and expression. *Gene Ther.* **2006**, *13* (7), 641–5.

(32) Boztug, K.; Dewey, R. A.; Klein, C. Development of hematopoietic stem cell gene therapy for Wiskott-Aldrich syndrome. *Curr. Opin. Mol. Ther.* **2006**, *8* (5), 390–5.

(33) Pfaffl, M. W. A new mathematical model for relative quantification in real-time RT-PCR. *Nucleic Acids Res.* **2001**, *29* (9), e45.

(34) Itoh, K.; Tezuka, H.; Sakoda, H.; Konno, M.; Nagata, K.; Uchiyama, T.; Uchino, H.; Mori, K. J. Reproducible establishment of hemopoietic supportive stromal cell lines from murine bone marrow. *Exp. Hematol.* **1989**, *17* (2), 145–53.

(35) Persons, D. A.; Baum, C. Solving the problem of gamma-retroviral vectors containing long terminal repeats. *Mol. Ther.* **2011**, *19* (2), 229–31.

(36) IDW Press Release: Effective gene therapy for children with Wiskott-Aldrich-syndrome. Nov 11, 2010.

(37) Zhou, S.; Mody, D.; DeRavin, S. S.; Hauer, J.; Lu, T.; Ma, Z.; Hacein-Bey Abina, S.; Gray, J. T.; Greene, M. R.; Cavazzana-Calvo, M.; Malech, H. L.; Sorrentino, B. P. A self-inactivating lentiviral vector for SCID-X1 gene therapy that does not activate LMO2 expression in human T cells. *Blood* **2010**, *116* (6), 900–8.

(38) Metcalf, J. A.; Ma, X.; Linders, B.; Wu, S.; Schambach, A.; Ohlemiller, K. K.; Kovacs, A.; Bigg, M.; He, L.; Tollefsen, D. M.; Ponder, K. P. A self-inactivating gamma-retroviral vector reduces manifestations of mucopolysaccharidosis I in mice. *Mol. Ther.* **2010**, *18* (2), 334–42.

(39) Marangoni, F.; Bosticardo, M.; Charrier, S.; Draghici, E.; Locci, M.; Scaramuzza, S.; Panaroni, C.; Ponzoni, M.; Sanvito, F.; Doglioni, C.; Liabeuf, M.; Gjata, B.; Montus, M.; Siminovitch, K.; Aiuti, A.; Naldini, L.; Dupre, L.; Roncarolo, M. G.; Galy, A.; Villa, A. Evidence for long-term efficacy and safety of gene therapy for Wiskott-Aldrich syndrome in preclinical models. *Mol. Ther.* **2009**, *17* (6), 1073–82.

(40) Galy, A.; Roncarolo, M. G.; Thrasher, A. J. Development of lentiviral gene therapy for Wiskott Aldrich syndrome. *Expert Opin. Biol. Ther.* **2008**, *8* (2), 181–90.

(41) Blundell, M. P.; Bouma, G.; Calle, Y.; Jones, G. E.; Kinnon, C.; Thrasher, A. J. Improvement of migratory defects in a murine model of Wiskott-Aldrich syndrome gene therapy. *Mol. Ther.* **2008**, *16* (5), 836–44.

(42) Modlich, U.; Navarro, S.; Zychlinski, D.; Maetzig, T.; Knoess, S.; Brugman, M. H.; Schambach, A.; Charrier, S.; Galy, A.; Thrasher, A. J.; Bueren, J.; Baum, C. Insertional Transformation of Hematopoietic Cells by Self-inactivating Lentiviral and Gammaretroviral Vectors. *Mol. Ther.* **2009**, *17* (11), 1919–28.

(43) Moreno-Carranza, B.; Gentsch, M.; Stein, S.; Schambach, A.; Santilli, G.; Rudolf, E.; Ryser, M. F.; Haria, S.; Thrasher, A. J.; Baum, C.; Brenner, S.; Grez, M. Transgene optimization significantly improves SIN vector titers, gp91(phox) expression and reconstitution of superoxide production in X-CGD cells. *Gene Ther.* **2009**, *16* (1), 111–8.

(44) Ng, Y. Y.; Baert, M. R.; Pike-Overzet, K.; Rodijk, M.; Brugman, M. H.; Schambach, A.; Baum, C.; Hendriks, R. W.; van Dongen, J. J.; Staal, F. J. Correction of B-cell development in Btk-deficient mice using lentiviral vectors with codon-optimized human BTK. *Leukemia* **2010**, *24* (9), 1617–30.

(45) Huston, M. W.; van Til, N. P.; Visser, T. P.; Arshad, S.; Brugman, M. H.; Cattoglio, C.; Nowrouzi, A.; Li, Y.; Schambach, A.; Schmidt, M.; Baum, C.; von Kalle, C.; Mavilio, F.; Zhang, F.; Blundell, M. P.; Thrasher, A. J.; Verstegen, M. M.; Wagemaker, G. Correction of Murine SCID-X1 by Lentiviral Gene Therapy Using a Codon-optimized IL2RG Gene and Minimal Pretransplant Conditioning. *Mol. Ther.* **2011**, DOI: 10.1038/mt.2011.127.

(46) Olivier, A.; Jeanson-Leh, L.; Bouma, G.; Compagno, D.; Blondeau, J.; Seye, K.; Charrier, S.; Burns, S.; Thrasher, A. J.; Danos, O.; Vainchenker, W.; Galy, A. A partial down-regulation of WASP is sufficient to inhibit podosome formation in dendritic cells. *Mol. Ther.* **2006**, *13* (4), 729–37.

(47) Schambach, A.; Swaney, W. P.; Loo, J. C. Design and production of retro- and lentiviral vectors for gene expression in hematopoietic cells. *Methods Mol. Biol.* **2009**, *506*, 191–205.